Spin reorientation and crystal-field interaction in $TbFe_{12-x}Ti_x$ single crystals

J. L. Wang, B. García-Landa, C. Marquina, and M. R. Ibarra
Departmento de Física de la Materia Condensada-ICMA, Facultad de Ciencias, Universidad de Zaragoza-CSIC, 50009 Zaragoza, Spain

F. M. Yang and G. H. Wu
State Key Laboratory of Magnetism, Institute of Physics, Chinese Academy of Sciences, P.O. Box 603, Beijing 100080, People's Republic of China

(Received 6 June 2002; published 22 January 2003)

The magnetic properties of $TbFe_{12-x}Ti_x$ single crystals with $x=0.8-1.4$ have been investigated in detail using ac and dc susceptibility and high-field magnetization measurements. A first-order spin reorientation transition from a basal plane easy magnetization direction at low temperatures to an axial easy magnetization direction at high temperatures occurs for all the investigated compounds. The spin reorientation temperatures have been determined by combining ac and dc susceptibility measurements and its dependence on both the Ti content and the applied magnetic field has been studied. A first-order magnetization process is observed below a certain temperature when the magnetic field is applied along the [001] crystallographic direction. The dependence of the transition critical field on the Ti content has been analyzed. The magnetic behavior has been interpreted using a two-sublattices model for the magnetic structure, in the frame of a crystal-electric-field–mean-field model. The parameters describing the crystal-field interaction in $TbFe_{12-x}Ti_x$ compounds have been determined. The calculated magnetic behavior shows a good agreement with experimental results in a wide temperature range.

DOI: 10.1103/PhysRevB.67.014417 PACS number(s): 75.10.Dg, 75.30.Cr, 75.30.Gw, 75.50.Gg

I. INTRODUCTION

In recent years, many studies have been undertaken to improve the magnetic properties of iron-based rare-earth (R) transition-metal (T) intermetallic compounds.[1] In particular, great attention has been paid to the $ThMn_{12}$-type R-T compounds due to their magnetic properties and simple crystal structure.[2] From a fundamental point of view, this series provides a good opportunity to study the crystal-field interaction in R-T intermetallic compounds. These compounds have a tetragonal structure (space group $I4/mmm$) with only one R site ($2a$) and three nonequivalent T sites ($8i$, $8j$, and $8f$). Several attempts have been made in order to explain the magnetic properties of these intermetallics from a microscopic point of view.[3–9] Of particular interest is the knowledge of the anisotropy arising from the rare-earth sublattice, which has its origin in the crystal-electric-field (CEF) interaction. The R-sublattice contribution to the magnetic anisotropy energy can be described in the frame of a single-ion CEF model, where the CEF interaction is described by the so-called CEF Hamiltonian, in which the CEF parameters B_n^m account for the intensity of such interaction.[8] The CEF parameters set can be determined by fitting different experimental results to the CEF model, such as magnetization measurements and inelastic neutron scattering. Moreover, the occurrence of the field- or temperature-induced magnetic transitions like spin reorientation transitions (SRT's) or first-order magnetization processes (FOMP's) can impose strong limitations on the values of the CEF parameters.[10,11] In the case of the $RFe_{11}Ti$ compounds there are some discrepancies with respect to the number and value of the CEF parameters necessary to describe the R anisotropy.[3,4,9] For example Hu *et al.* have obtained a set of five CEF parameters by fitting the experimental magnetization data of $DyFe_{11}Ti$ single crystal, but they cannot account for the magnetic behavior of $TbFe_{11}Ti$ compound.[3]

Considerable confusion also exists about the magnetic structures occurring in the $RFe_{11}Ti$ compounds at various temperatures and about the nature of the magnetic phase transitions. In particular for $TbFe_{11}Ti$, very large discrepancies do exist with regard to the spin reorientation transition.[12–14] In a previous work these differences were ascribed to the fact that the temperature and character of the SRT are very sensitive to the applied magnetic field.[15] Rather fewer investigations of the composition influence on magnetic properties in $RFe_{12-x}Ti_x$ compounds have been reported. Generally speaking, the Curie temperature T_C is very sensitive to the composition in the R-T compounds, and can be regarded as a parameter to compare the possible differences in composition. However, our recent investigation on $RFe_{12-x}Nb_x$ compounds clearly indicated that a slight change of the Nb concentration in $DyFe_{12-x}Nb_x$ and $TbFe_{12-x}Nb_x$ compounds can lead to a pronounced shift of the spin reorientation temperature even though T_C keeps almost constant.[16] Therefore, in order to explain the discrepancies reported in the literature about spin reorientation transition in $TbFe_{11}Ti$, it is necessary to further investigate, in $TbFe_{12-x}Ti_x$ compounds, the influence of the chemical composition and/or other external conditions on the anisotropy. Compared to polycrystalline samples, single-crystalline samples enable a more precise observation of magnetic transitions and provide more accurate information from the magnetic measurements. It is well known that the ac susceptibility depends on the magnetic anisotropy. Therefore, the measurement of the temperature dependence of the complex susceptibility, $\chi_{ac}=\chi'-j\chi''$ can be used to detect the temperature-induced magnetic transitions caused by the

change of the magnetic anisotropy energy in the *R-T* compounds.[17]

In this paper, a detailed investigation of spin reorientation transitions and first-order field-induced transitions in various $TbFe_{12-x}Ti_x$ single crystals using ac and dc susceptibility measurements and high-field magnetization measurements is presented. Moreover, the magnetic behavior of some $TbFe_{12-x}Ti_x$ compounds is analyzed from a microscopic point of view in a wide temperature range using a single-ion exchange and CEF interaction model, which constitutes a very strict test of validity of the model used and also guarantees the reliability of the determined parameters.

II. EXPERIMENTAL METHODS

The magnetization and ac susceptibility have been measured on $TbFe_{12-x}Ti_x$ single-crystalline samples with $x = 0.8-1.4$. The samples were grown by the Czochralski technique with a cold crucible, and cut in the Institute of Physics, Chinese Academy of Science. Details of the preparation and quality of the single crystals can be found in Ref. 18. High-field magnetization measurements were performed in the Van der Waals-Zeeman Institute, University of Amsterdam. The $YFe_{12-x}Ti_x$ polycrystals have been prepared by argon arc melting the constituent elements with purities of at least 99.9%. The ingots were wrapped in molybdenum foil and sealed in quartz tubes, followed by annealing in vacuum at 1273 K for 72 h, and then quenched in water. In order to obtain magnetically aligned samples, fine-powdered particles of the $YFe_{12-x}Ti_x$ compounds were mixed with epoxy resin and filled in two plastic tubes of cylindrical shape. The plastic tubes were placed in an external magnetic field of about 1.0 T with their cylindrical axis either parallel or perpendicular to the field direction, respectively, until the epoxy resin solidifies. The ac susceptibility measurements were performed in a superconducting quantum interference device with an ac field of 4.5 Oe and frequencies of 10 and 100 Hz. In the present investigation, various dc fields have been applied.

III. EXPERIMENTAL RESULTS

Both x-ray-diffraction measurements and thermomagnetic analysis show that all $TbFe_{12-x}Ti_x$ single crystals and $YFe_{12-x}Ti_x$ polycrystals are single phase, and crystallize in a $ThMn_{12}$-type structure. As an example, the $M(T)$ curves obtained for some selected $TbFe_{12-x}Ti_x$ single crystals under a low magnetic field applied along the [001] crystallographic direction are shown in Fig. 1. It can be seen that T_C presents an almost composition-independent value (554 K), while the spin reorientation temperature T_{sr} rapidly increases with decreasing Ti content. The composition dependence of T_{sr} and T_C in $TbFe_{12-x}Ti_x$ is similar to the measured on $DyFe_{12-x}Nb_x$ and $TbFe_{12-x}Nb_x$ polycrystals.[16] It can be observed that the decreasing rate of T_{sr} with increasing Ti content is larger than 300 K/Ti. This fact could explain the contradictory reports on the T_{sr} values for $TbFe_{11}Ti$ in previous references, which may result from possible differences in chemical composition of the samples except for the case of the field influence described in Ref. 12.

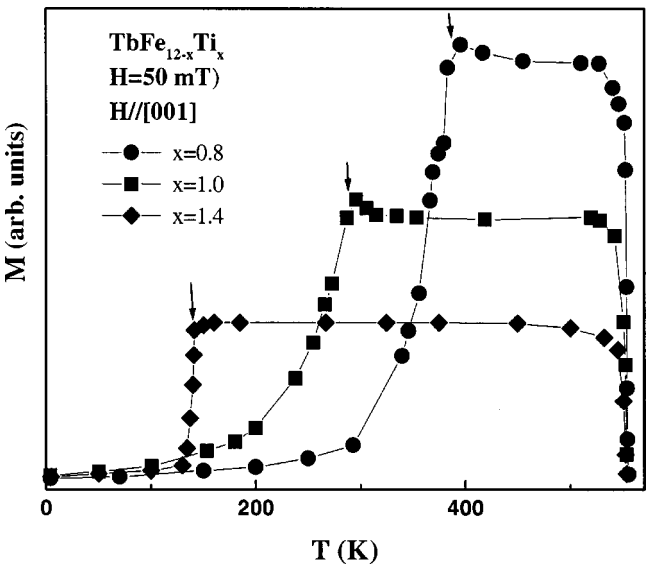

FIG. 1. Temperature dependence of the magnetization measured on $TbFe_{1-x}Ti_x$ single crystals when the field is applied along the [001] crystallographic direction. T_{sr} is marked by arrows.

Figures 2(a) and 2(b) show the temperature dependence of the real (χ') and imaginary (χ'') components of the ac susceptibility of $TbFe_{10.7}Ti_{1.3}$ when the ac ($\mathbf{h}_{ac}$) and dc ($\mathbf{H}$) fields are applied parallel [Fig. 2(a)] or perpendicular [Fig. 2(b)] to the [001] direction, for several values of the dc field. For highly anisotropic materials, the value of χ' is determined mainly by the magnetic anisotropy energy and the domain-wall energy, whereas the value of χ'' gives the energy absorption by the compound. It can be seen that a pronounced anomaly occurs in both χ'-T and χ''-T curves at about 200 K at zero dc field. In this case, when $\mathbf{h}_{ac}$ is applied along the [001] direction the shape of the anomaly in both χ' and χ'' curves is steplike, whereas when the $\mathbf{h}_{ac}$ field is perpendicular to [001] the anomaly becomes peaklike. According to magnetization measurements performed on single crystals when an external field is applied along different crystallographic directions at different temperatures, it can be concluded that the anomaly in both χ' and χ'', as well as the one observed in the $M(T)$ measurements, is due to a spin reorientation transition, in which the easy magnetization direction (EMD) changes from the basal plane ($T<T_{sr}$) to the c axis ($T>T_{sr}$). In the literature the experimental definition of T_{sr} from the $\chi'(T)$ curves is somewhat controversial. Some authors assign T_{sr} to the inflection point (i.e., a minimum of $d\chi'/dT$),[9,19,20] while other authors place T_{sr} at the χ' vs T maximum.[7,21,22] Here we have adopted the latest definition. Therefore T_{sr} for $TbFe_{10.7}Ti_{1.3}$ is determined to be 205 K (± 5 K). Under a nonzero applied dc field, the values of both χ' and χ'' rapidly decrease and the shape of the anomaly in both $\chi'(T)$ and $\chi''(T)$ becomes peaklike even for the curves obtained with $\mathbf{h}_{ac}$ parallel to [001] [see Fig. 2(a)]. The position of the peak in both χ' and χ'' shifts to lower temperatures when $\mathbf{H}$ is applied along the [001] direction and to higher temperatures when $\mathbf{H}$ is applied perpendicular to the [001] direction. This effect means that although

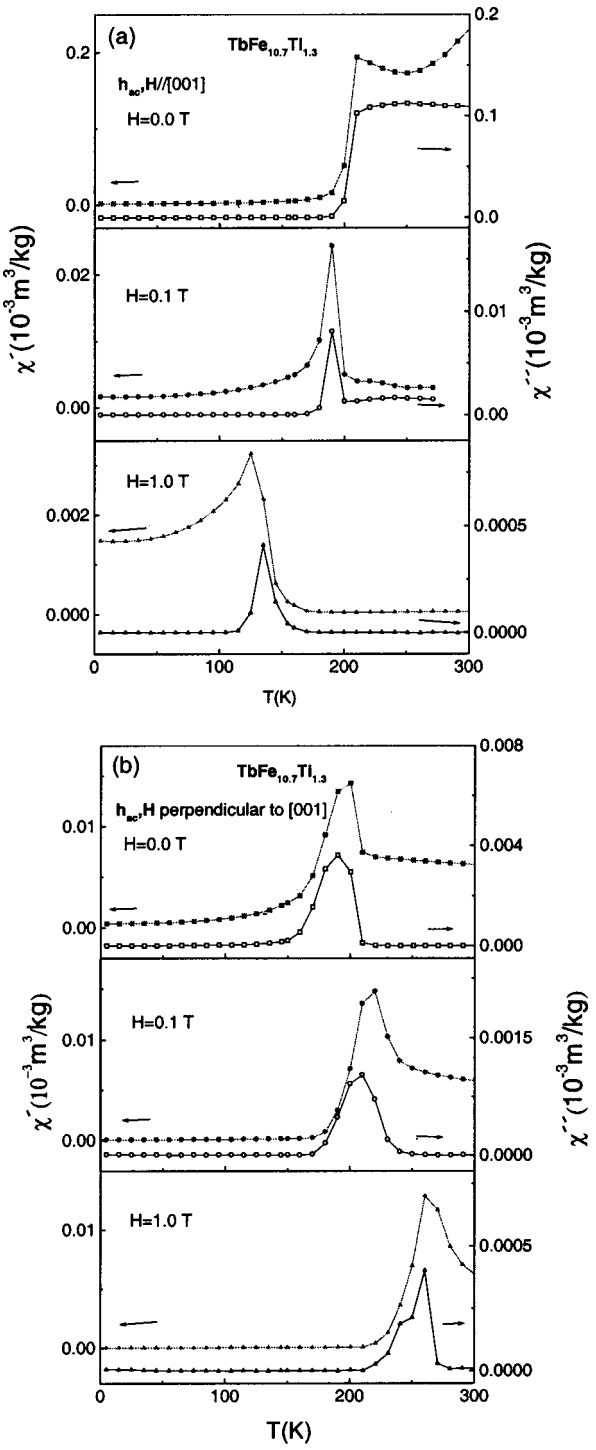

FIG. 2. Temperature dependence of the real, χ', and imaginary (χ'') components of the ac susceptibility, when $\mathbf{h}_{ac}$ and $\mathbf{H}$ are applied parallel (a) or perpendicular (b) to the [001] direction in a $TbFe_{10.7}Ti_{1.3}$ single crystal, for several values of H. ($h_{ac}=4.5$ Oe and $f=100$ Hz)

the Zeeman energy produced by the applied external dc field keeps the magnetization parallel to the field direction, the application of an external dc field modifies T_{sr}: it increases 75 K when the **H** is applied parallel to the [001] direction, whereas T_{sr} decreases 60 K when the **H** is applied perpendicular to the [001] direction. This implies that the anisotropy energy is comparable with the Zeeman energy produced by a 1.0-T applied magnetic field. As shown in Sec. IV this assumption will be confirmed by our CEF analysis.

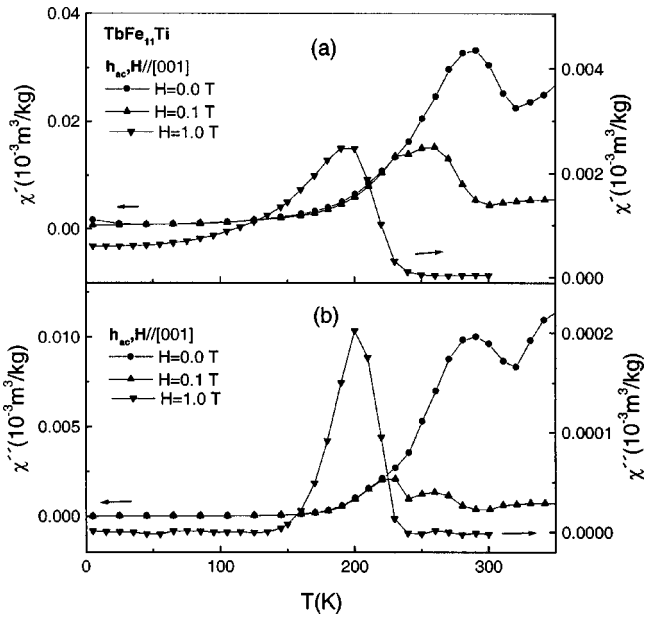

FIG. 3. Temperature dependence of the χ' (a) and χ'' (b) parts of the ac susceptibility for a $TbFe_{11}Ti$ single crystal and values of $\mathbf{h}_{ac}$ and $\mathbf{H}$. In all the cases $h_{ac}=4.5$ Oe and $f=100$ Hz.

The temperature dependence of χ' and χ'' in the case of the $TbFe_{11}Ti$ single crystal when the $\mathbf{h}_{ac}$ and $\mathbf{H}$ are applied along the [001] direction, for several values of the dc field is shown in Figs. 3(a) and 3(b), respectively. The observed peaklike anomalies at $H=0$ indicate that a SRT occurs at about $T_{sr}=285$ K, confirming the results obtained by Zhang *et al.*[14] According to magnetization measurements the EMD changes from an easy-plane EMD at low temperature to an easy-axis EMD at high temperature. Compared with $TbFe_{10.7}Ti_{1.3}$, the peak corresponding to the SRT anomaly in both $\chi'(T)$ and $\chi''(T)$ curves is more round in the present compound. When a dc field of 1.0 T is applied along the [001] direction T_{sr} decreases to 193 K (this decrease is larger than that for $TbFe_{10.7}Ti_{1.3}$). This dependence of T_{sr} on the value and direction of the applied magnetic field can be the origin of the very large discrepancies with regard to the type of spin reorientation and the value of T_{sr} reported for $TbFe_{11}Ti$ compound mentioned in Sec. I (see Ref. 15 for a summary). In the $M(T)$ curves a similar tendency for the variation of T_{sr} under applied field has been observed in single crystal[15] and in polycrystalline samples.[9]

Figures 4(a) and 4(b) display the results for $\chi'(T)$ and $\chi''(T)$, respectively, obtained on a $TbFe_{11.15}Ti_{0.85}$ single crystal with the ac field applied along the [001] direction in various dc fields. T_{sr} is derived to be 340 K at zero dc field. With an increasing dc field the shape of both $\chi'(T)$ and $\chi''(T)$ curves becomes much sharper. A 1.0-T dc field applied along the [001] direction shifts T_{sr} to 238 K. The effect of the ac frequency changes from 100 to 10 Hz on T_{sr} has also been studied, but no influence on either $\chi'(T)$ or $\chi''(T)$ curves has been observed.

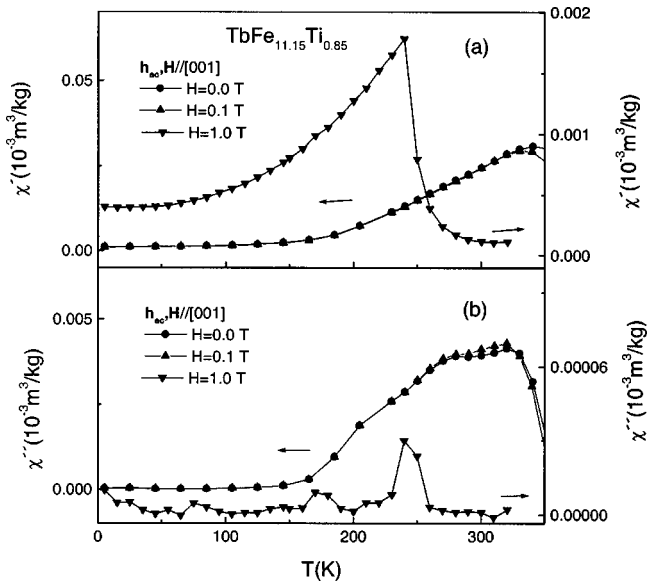

FIG. 4. Temperature dependence of the χ' (a) and χ'' (b) parts of the ac susceptibility for a $TbFe_{11.15}Ti_{0.85}$ single crystal in various dc fields. ($h_{ac}=4.5$ Oe and $f=100$ Hz).

The magnetization isotherms, obtained when the field is applied along the [001] direction for $TbFe_{10.7}Ti_{1.3}$, are shown in Fig. 5. A jump in the magnetization takes place below 210 K, being more evident at low temperatures (the magnetization value at 1.5 K changes from $5.5\mu_B$/f.u. at 3.5 T to $10.4\mu_B$/f.u. at 4.2 T). This particular field dependence of the magnetization and its similarity with the observed in

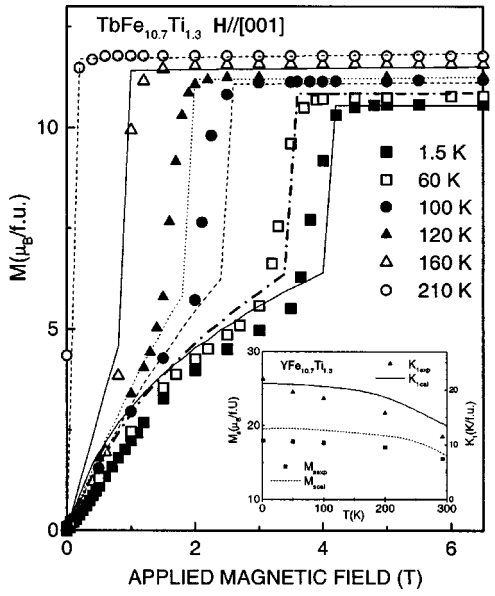

FIG. 5. Magnetization isotherms of $TbFe_{10.7}Ti_{1.3}$ when the magnetic field is applied along the [001] direction. The symbols correspond to the experimental data and the lines represent the calculation for the parameters set collected in Table I. Inset: temperature variation of the iron anisotropy constant K_1 and the iron magnetization M_s. Symbols are the experimental values obtained from the $YFe_{10.7}Ti_{1.3}$ polycrystal. Lines are the theoretical calculation using the parameters listed in Table I.

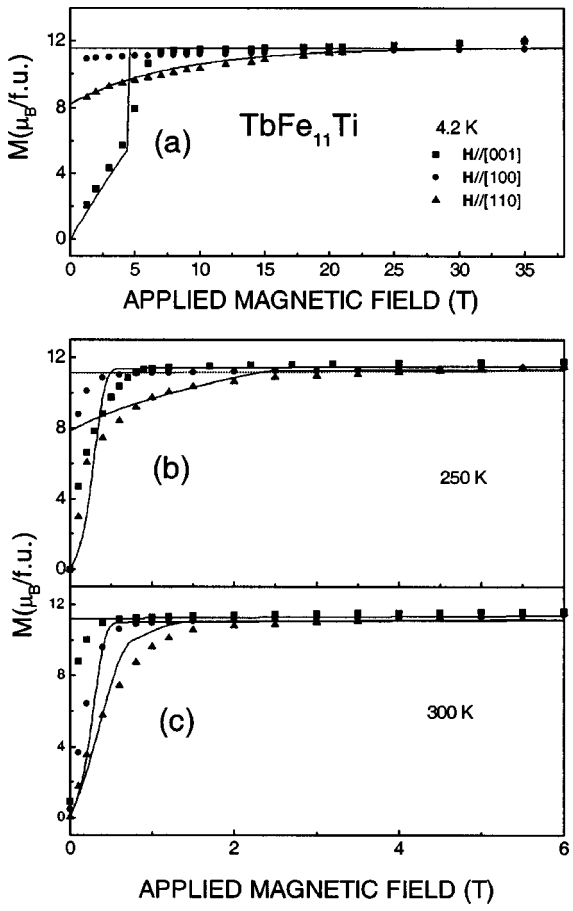

FIG. 6. Magnetization isotherms of $TbFe_{11}Ti$ obtained when the magnetic field is applied along the crystallographic axes [100], [110], and [001]. Full lines are the theoretical curves obtained using the parameters listed in Table I.

other $ThMn_{12}$ compounds,[4,9] points to the existence of a FOMP-like transition. It can also be seen that the critical field at which this transition takes place decreases with increasing temperature.

The magnetization isotherms obtained for $TbFe_{11}Ti$ and $TbFe_{11.15}Ti_{0.85}$ under an applied field along the different crystallographic directions at some selected temperatures are shown in Figs. 6 and 7, respectively. It can be seen that the transition critical field at 4.2 K shifts from 3.5 T for $x=1.3$ to 4.4 T for $x=1.0$, and to 10.0 T for $x=0.85$.

IV. ANALYSIS

To interpret the observed behavior we will work in the frame of an ionic CEF model. In order to account for the total free energy of a compound we will consider two main contributions: the *R*-sublattice contribution and the Fe-sublattice one. The *R*-sublattice contribution can be calculated from the Hamiltonian describing the magnetic properties of the R^{3+} ions in the tetragonal $RFe_{12-x}Ti_x$ compounds in the presence of an internal magnetic field $\boldsymbol{H_i}$. It can be written as

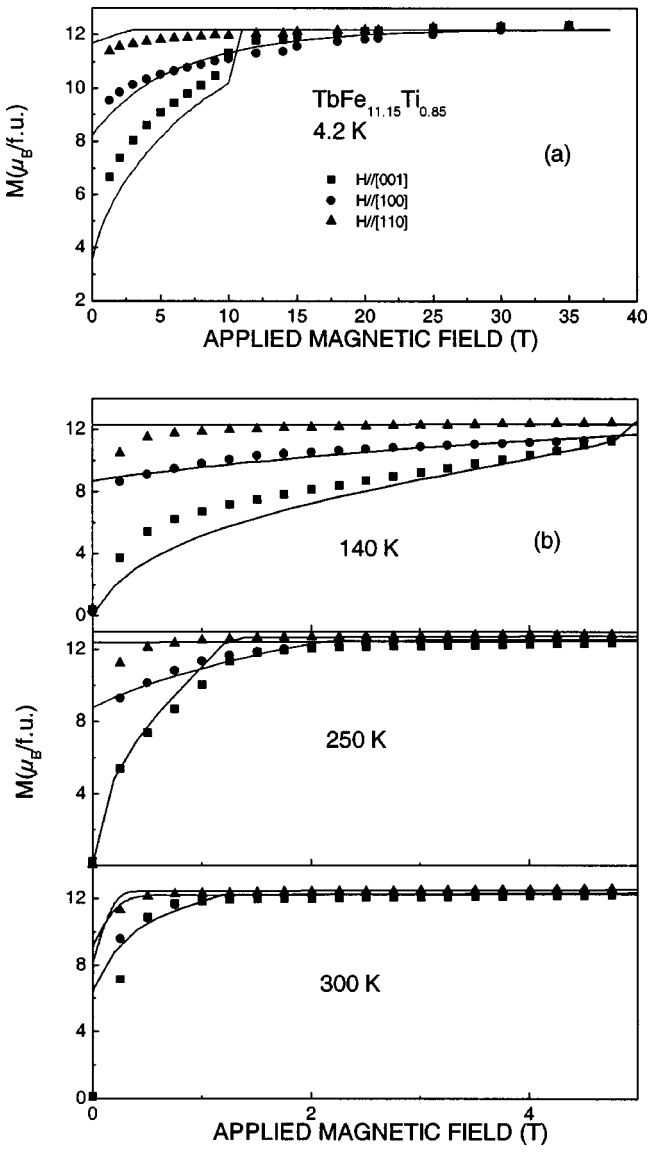

FIG. 7. Magnetization isotherms of $TbFe_{11.15}Ti_{0.85}$ obtained when the magnetic field is applied along the crystallographic axes [100], [110], and [001]. Full lines are the theoretical curves obtained using the parameters listed in Table I.

$$H = H_{\mathrm{CEF}} + 2(g_J - 1)\mu_B \boldsymbol{J} H_{\mathrm{ex}}(T) + g_J \mu_B \boldsymbol{J} \boldsymbol{H_i}, \qquad (1)$$

where H_{CEF} represents the CEF Hamiltonian, which describes the CEF interaction at the rare earth site. As noted in Sec. I, a knowledge of this interaction is of fundamental importance for understanding the *R*-sublattice anisotropic behavior. The CEF Hamiltonian at the rare-earth $2a$ sites in the $ThMn_{12}$-type structure can be expressed as

$$H_{\mathrm{CEF}} = B_2^0 O_{20} + B_4^0 O_{40} + B_4^4 O_{44} + B_6^0 O_{60} + B_6^4 O_{64}, \qquad (2)$$

where the B_n^m are the CEF parameters and the O_{nm} are the CEF Stevens operators.[8] The second term of Eq. (1) represents the $3d$-$4f$ exchange interaction, which can be expressed, within the mean-field approximation, by an effective exchange magnetic field $\boldsymbol{H_{ex}}(T)$, considered proportional in magnitude and antiparallel to the iron sublattice magnetization: $H_{\mathrm{ex}}(T) = H_{\mathrm{ex}}(0)[M_{\mathrm{Fe}}(T)/M_{\mathrm{Fe}}(0)]$. $\boldsymbol{J}$ is the R^{3+} total angular momentum and g_J the Landé factor. The last term of Eq. (1) describes the Zeeman interaction of the R^{3+} sublattice under an internal field $\boldsymbol{H_i}$.

The magnetic free energy of the R^{3+} sublattice is obtained from the canonical partition function $Z_R = \Sigma_n \exp(-E_n/k_B T)$ where E_n are the eigenvalues of the Hamiltonian given by expression (1). The free energy of the rare-earth sublattice is given by

$$F^R(\theta, \varphi, \theta_H, \varphi_H, H_i, T) = -k_B T \ln Z_R, \qquad (3)$$

where H_i is the magnitude of the internal field, θ_H and φ_H are the spherical angles determining the direction of $\boldsymbol{H_i}$, and θ and φ are the spherical angles for the exchange mean-field ($\boldsymbol{H_{ex}}$) direction.

The total free energy is calculated by adding to F_R the uniaxial Fe sublattice anisotropy free energy together with the Zeeman interaction for the Fe sublattice, i.e.,

$$\begin{aligned} F(\theta, \varphi, \theta_H, \varphi_H, H_i, T) &= -k_B T \ln Z_R + K_1(T)\sin^2\theta - M_{\mathrm{Fe}}(T) H_i [\sin\theta \sin\theta_H \\ &\quad \times \cos(\varphi_H - \varphi) + \cos\theta \cos\theta_H], \end{aligned} \qquad (4)$$

where $M_{\mathrm{Fe}}(T)$ and $K_1(T)$ represent the thermal variation of the magnetization and anisotropy constant of the Fe sublattice, respectively, determined from the corresponding $YFe_{12-x}Ti_x$ compound and scaled to the Curie temperature of the corresponding $TbFe_{12-x}Ti_x$ compounds.[3,9] The magnetic structure at any given temperature and applied magnetic field is determined by the exchange mean-field equilibrium angles θ_0 and φ_0, which minimize the total free energy given by Eq. (4).

The process of determination of the CEF parameters from the magnetization results in the present work follows the procedure described in Ref. 10, taking into account the restrictive conditions imposed by the occurrence of a FOMP-like transition and of a SRT. For determining the CEF parameters we have proceeded as follows. First we consider an experimental magnetization isotherm $M_{\mathrm{expt}}(T_1)$ obtained at low temperature T_1 (for example, $T_1 = 1.5$ K for $TbFe_{10.7}Ti_{1.3}$). Given a certain parameter set, if the calculated magnetization $M_{\mathrm{cal}}(T_1)$ lies for the measured field range within a reasonable error bar $M_{\mathrm{expt}} \pm \Delta M_{\mathrm{expt}}$, then the set is considered for further analysis. In this way we obtain several $\{B_n^m\}$ sets associated with temperature T_1. In the following steps the number of possible solutions is reduced gradually by means of imposing the restrictions given by other higher-temperature experimental isotherms $M_{\mathrm{expt}}(T_2)$, $M_{\mathrm{expt}}(T_3)$, etc. Due to the large number of parameters involved in the calculation we did not find a unique solution. Several sets of parameters give acceptable fits to all the experimental data. Among them we have considered the set which leads to the best fit of the experimental data. The CEF parameters determined by the fitting procedure for $TbFe_{10.7}Ti_{1.3}$, $TbFe_{11}Ti$, and $TbFe_{11.15}Ti_{0.85}$ are listed in Table I. Due to the fact that for the $TbFe_{10.7}Ti_{1.3}$ compound we could only analyze the magnetization isotherms along the [001] direction, the values

TABLE I. Crystal field B_n^m parameters (in units of K/ion), $\mu_B H_{ex}(0)$ (in K units), at 0 K obtained from fitting the single-crystal magnetization curves of $TbFe_{10.7}Ti_{1.3}$, $TbFe_{11}Ti$, and $TbFe_{11.15}Ti_{0.85}$. A_n^m are the corresponding crystal-field coefficients (in units of Ka_0^{-n}): $A_n^m = B_n^m/\theta_n\langle r^n\rangle$, $\{\theta_n\}$ are the Stevens coefficients, and the $\langle r^n\rangle$ represent the Hartree-Fock radial intergrals.

$TbFe_{10.7}Ti_{1.3}$	B_2^0	B_4^0	B_4^4	B_6^0	B_6^4	$\mu_B H_{ex}(0)$
	0.40 ± 0.02	$(-7.2\pm2)\times10^{-4}$	$(-90\pm10)\times10^{-4}$	$(-21\pm7)\times10^{-6}$	0	126
	A_2^0	A_4^0	A_4^4	A_6^0	A_6^4	
	-48 ± 2.5	-3.56 ± 1	-44 ± 5	2.73 ± 0.9	0	
$TbFe_{11}Ti$	B_2^0	B_4^0	B_4^4	B_6^0	B_6^4	$\mu_B H_{ex}(0)$
	0.43 ± 0.02	$(-11\pm3)\times10^{-4}$	$(-140\pm15)\times10^{-4}$	$(-3.8\pm1.4)\times10^{-6}$	0	149.5
	A_2^0	A_4^0	A_4^4	A_6^0	A_6^4	
	-51.8 ± 2.4	-5.4 ± 1.5	-69.3 ± 7.5	0.49 ± 0.2	0	
$TbFe_{11.15}Ti_{0.85}$	B_2^0	B_4^0	B_4^4	B_6^0	B_6^4	$\mu_B H_{ex}(0)$
	0.45 ± 0.02	$(7.3\pm2)\times10^{-4}$	$(130\pm15)\times10^{-4}$	$(-18\pm6)\times10^{-6}$	0	150.2
	A_2^0	A_4^0	A_4^4	A_6^0	A_6^4	
	-54.2 ± 2.4	3.61 ± 1	64.32 ± 7.4	2.34 ± 0.8	0	

of B_4^4 and B_6^4 for this compound have to be taken with certain reservations. The calculated $M(H)$ curves for these compounds are drawn by solid lines in Figs. 5, 6, and 7. In all the cases it can be seen that the obtained parameters sets account quite well for the experimental results.

In the inset of Fig. 5, the thermal variation of the magnetization M_s at zero field and the anisotropy constant K_1 of $YFe_{10.7}Ti_{1.3}$, together with the curves used in the fitting for the Fe-sublattice contribution, are shown. The calculated spin reorientation temperature in absence of an external applied field is 215 K which agrees well with the data obtained from ac susceptibility measurement.

In the case of for $TbFe_{11}Ti$ the magnetization isotherms shown in Fig. 6 show that the magnetic anisotropy within the (001) plane is very large, and that the magnetic field needed to saturate the magnetization along the [110] direction is larger than the one needed to saturate along the [001] direction. A similar behavior was observed in a $DyFe_{11}Ti$ single crystal.[3] In a phenomenological way the anisotropy of Tb^{3+} ion in these compounds can be described by the expression[23]

$$E_{Tb}^a = K_1(Tb)\sin^2\theta + [K_2(Tb) + K_2'(Tb)\cos 4\phi]\sin^4\theta + [K_3(Tb) + K_3'(Tb)\cos 4\phi]\sin^6\theta, \quad (5)$$

where θ and ϕ are the polar angles of the magnetization vector in a reference frame where **x** is parallel to [100] and **z** is parallel to [001]. The anisotropy energy between [110] and [100] in the basal plane can be written as

$$\Delta E = E_{[110]} - E_{[100]} = -2[K_2'(Tb) + K_3'(Tb)]. \quad (6)$$

The relationship between the anisotropy constants $\{K_i\}$ for the rare-earth and crystal-field parameters, $\{B_n^m\}$, can be obtained by a rotation transformation of crystal-field terms:[23,24]

$$K_1(R) = -[\tfrac{3}{2}B_{20}\langle O_{20}\rangle + 5B_{40}\langle O_{40}\rangle + \tfrac{21}{2}B_{60}\langle O_{60}\rangle],$$

$$K_2(R) = \tfrac{7}{8}[5B_{40}\langle O_{40}\rangle + 27B_{60}\langle O_{60}\rangle],$$

$$K_2'(R) = \tfrac{1}{8}[B_{44}\langle O_{40}\rangle + 5B_{64}\langle O_{60}\rangle], \quad (7)$$

$$K_3(R) = -\tfrac{231}{16}B_{60}\langle O_{60}\rangle,$$

$$K_3'(R) = -\tfrac{11}{16}B_{64}\langle O_{60}\rangle.$$

The planar anisotropy is originated from the interplay of K_2' and K_3' which are determined by $B_4^4\langle O_{40}\rangle$ and $B_6^4\langle O_{60}\rangle$. The CEF parameters are related to the CEF coefficients A_n^m by the expression $B_n^m = \theta_n A_n^m\langle r^n\rangle$, where θ_n are the Stevens coefficients and $\langle r^n\rangle$ represent the Hartree-Fock radial integrals.[8] According to Eq. (4), the larger planar anisotropy implies that A_4^4 and A_6^4 should take a rather large value compared with other two coefficients A_4^0 and A_6^0. For $TbFe_{11}Ti$ and $TbFe_{11.15}Ti_{0.85}$, one obtains $B_4^4\langle O_{40}\rangle = -83.1$ K, $B_6^4\langle O_{60}\rangle = -10.3$ K, and $B_4^4\langle O_{40}\rangle = 77.2$ K and $B_6^4\langle O_{60}\rangle = 18.3$, respectively. Since the values of $B_6^4\langle O_{60}\rangle$ are much smaller than those of $B_4^4\langle O_{40}\rangle$, the planar anisotropy is actually dominated by the $B_4^4\langle O_{40}\rangle$. This fact is also true for Hu and co-workers' CEF parameters.[3,24]

It can be seen from Figs. 6 and 7 that at low temperatures the planar anisotropy changes dramatically when the Ti content increases from $x = 0.85$ to 1.0. At 5 K the EMD in the basal plane changes from [100] for $x = 1.0$ to [110] for $x = 0.85$ which is reflected from the change of the sign in B_4^4, as shown in Table I. Because A_n^m are proportional to the electric field gradient (EFG) at the R sites, due to the nearest-neighbor atoms at the $8i$ sites, substitution of Fe by Ti at

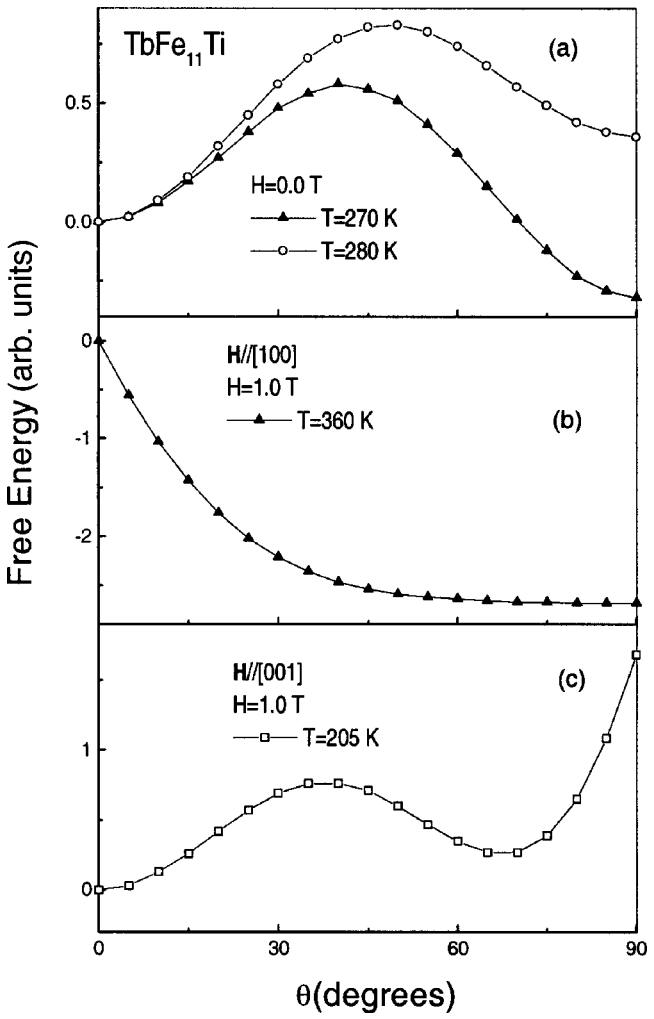

FIG. 8. Calculated free energy in the (100) plane for $TbFe_{11}Ti$ for several orientations of the applied magnetic field. θ is the angle between the EMD and the [001] direction.

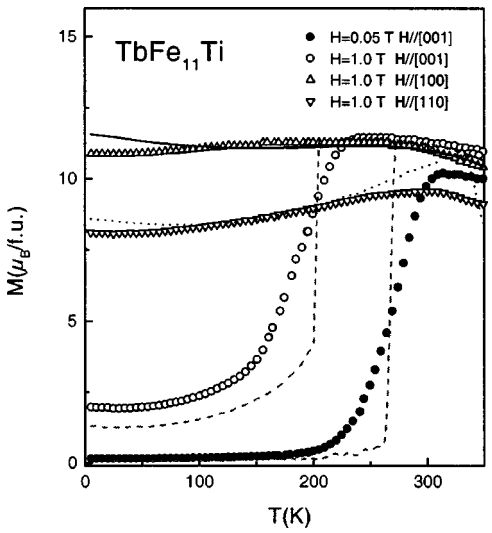

FIG. 9. Temperature dependence of the magnetization of $TbFe_{11}Ti$ for several applied magnetic fields. The symbols correspond to the experimental data and the lines represent the calculation for the parameters set listed in Table I.

these sites causes a modification of the EFG. Therefore, it may be expected that, with increasing Ti content, A_4^4 may decrease and change its sign at a certain x, leading to the abovementioned change of the B_4^4 sign (for Tb, $\beta_J>0$) and to the observed SRT within the (001) plane. The calculated T_{sr} using the CEF parameters listed in Table I are 270 and 320 K for $TbFe_{11}Ti$ and $TbFe_{11.15}Ti_{0.85}$, respectively.

In order to study the influence of an applied magnetic field on the spin reorientation temperature, we have calculated the free energy in the (100) and (110) planes ($\varphi_0=0°$ and $\varphi_0=45°$, respectively) at selected temperatures using the parameters set listed in Table I. As an example, the free energy in the (100) plane under various applied fields at the temperatures near T_{sr} is shown in Fig. 8 for the $TbFe_{11}Ti$ compound. It can be seen that under zero field [Fig. 8(a)] the free energy minimum shifts from $\theta_0=90°$ at 270 K to 0° at 280 K. This means that the EMD jumps from in the c plane at 270 K to along the c axis at 280 K. When a 1.0-T field is applied along the [100] direction the EMD still lies in the c plane even when temperature increases up to 360 K [see Fig. 8(b)]. Conversely, when such a field is applied along the [001] direction T_{sr} shifts to 205 K, as shown in Fig. 8(c). These theoretical predictions for the T_{sr} behavior account well for the experimental results displayed in Fig. 3.

We have also calculated the temperature dependence of the magnetization when the magnetic field is applied along different crystallographic directions, using the CEF parameters listed in Table I. As an example, the experimental and calculated results for $TbFe_{11}Ti$ are shown in Fig. 9. The good agreement between the experimental and calculated data confirms the reliability of the obtained parameters. This is also the case of the other two compounds.

V. CONCLUSIONS

In the present paper, a detailed study of the magnetic properties of $TbFe_{12-x}Ti_x$ single crystals is presented by means of ac and dc susceptibility and high-field magnetization measurements. A FOMP-like transition has been observed at low temperatures along the [001] direction for compounds with $x=0.85$, 1.0, and 1.3. The transition critical field at 5 K decreases with increasing Ti content. A SRT has been also observed, in which the EMD changes from lying on the basal plane at low temperatures to be parallel to the c axis at high temperatures. T_{sr} decreases dramatically with increasing Ti content and is very sensitive to an external applied magnetic field. This result helps to clarify the confusion about the magnetic structures occurring in the $RFe_{11}Ti$ compounds at different temperatures, as well as about the nature of the field-induced magnetic transitions. The magnetic behavior has been analyzed in a wide temperature range using a two-sublattice approximation for the magnetic structure. Within this approximation the Fe sublattice contribution to the free energy has been considered phenomenologically, whereas a single-ion CEF model has been used to

describe the R sublattice contribution. The parameters B_2^0, B_4^0, B_6^0, B_4^4, and B_6^4, describing the crystal-field interaction in $TbFe_{12-x}Ti_x$ compounds, have been determined. The calculated magnetic behavior shows a good agreement with the experimental data. The fact that our model fulfils the strict conditions imposed by the existence of the SR- and FOMP-like transitions confirms the reliability of the model and of the obtained CEF parameters sets.

ACKNOWLEDGMENTS

J.L.W. wishes to express his gratitude to the financial support of the Spanish CICYT under a grant.

[1] H. S. Li and J. M. D. Coey, in *Handbook of Magnetic Materials*, edited by K. H. J. Buschow (North-Holland, Amsterdam, 1991), Vol. 6, p. 1.
[2] K. H. J. Buschow, Rep. Prog. Phys. **549**, 1123 (1991).
[3] B. P. Hu, H. S. Li, J. M. D. Coey, and J. P. Gavigan, Phys. Rev. B **41**, 2221 (1990).
[4] C. Abadía, P. A. Algarabel, B. García-Landa, M. R. Ibarra, A. Del Moral, N. V. Kudrevatykh, and P. E. Markin, J. Phys.: Condens. Matter **10**, 349 (1998).
[5] L. M. García, J. Bartolomé, P. A. Algarabel, M. R. Ibarra, and M. D. Kuz'min, J. Appl. Phys. **73**, 5908 (1993).
[6] P. A. Algarabel, M. R. Ibarra, J. Bartolomé, L. M. García, and M. D. Kuz'min, J. Phys.: Condens. Matter **6**, 10 551 (1994).
[7] L. C. C. M. Nagamine, H. R. Rechenberg, P. A. Algarabel, and M. R. Ibarra, Phys. Rev. B **50**, 12 659 (1994).
[8] M. T. Hutchings, *Solid State Physics* (Academic, New York, 1964), Vol. 16, p. 227.
[9] X. C. Kou, T. S. Zhao, R. Grossinger, H. R. Kirchmayer, X. Li, and F. R. de Boer, Phys. Rev. B **47**, 3231 (1993).
[10] B. García-Landa, M. R. Ibarra, and P. A. Algarabel, Phys. Rev. B **51**, 15 132 (1995); B. García-Landa, P. A. Algarabel, M. R. Ibarra, F. E. Kayzel, and J. J. M. Franse, *ibid.* **55**, 8313 (1997).
[11] T. S. Zhao, H. M. Jin, G. H. Guo, X. F. Han, and H. Chen, Phys. Rev. B **43**, 8593 (1991).
[12] B. Hu, H. S. Li, J. P. Gavigan, and J. M. D. Coey, J. Phys.: Condens. Matter **1**, 755 (1989).
[13] L. Y. Zhang, E. B. Boltich, V. K. Sinha, and W. E. Wallace, IEEE Trans. Magn. **25**, 3303 (1989).
[14] L. Y. Zhang, B. M. Ma, Y. Zeng, and W. E. Wallace, J. Appl. Phys. **70**, 6119 (1991).
[15] A. V. Andreev, N. V. Kudrevatykh, S. M. Razgonyaev, and E. N. Tarasov, Physica B **183**, 379 (1993).
[16] J. L. Wang, N. Tang, Y. P. Shen, D. Yang, B. Fuquan, G. H. Wu, F. M. Yang, F. R. de Boer, E. Brück, and K. H. J. Buschow, J. Appl. Phys. **91**, 2165 (2002).
[17] X. C. Kou, T. S. Zhao, R. Grossinger, and F. R. de Boer, Phys. Rev. B **46**, 6225 (1992).
[18] G. H. Wu, B. P. Hu, S. X. Gao, Y. X. Li, J. Du, C. C. Tang, K. C. Jia, and W. S. Zhan, J. Cryst. Growth **192**, 417 (1998).
[19] P. Stefanski and A. Kowalezyk, Solid State Commun. **77**, 397 (1991).
[20] Z. H. Cheng, B. G. Shen, Q. W. Yan, H. Q. Guo, D. F. Chen, C. Gou, K. Sun, F. R. de Boer, and K. H. J. Buschow, Phys. Rev. B **57**, 14 299 (1998).
[21] Y. P. Shen, X. Y. Yin, N. Tang, J. L. Wang, D. Yang, W. H. Wang, G. H. Wu, F. M. Yang, and X. P. Zhong, J. Phys.: Condens. Matter **12**, 10 571 (2000).
[22] M. Foldeak, L. Koszgi, and R. A. Dunlap, J. Appl. Phys. **69**, 5562 (1991).
[23] C. Rudowiz, J. Phys. C **18**, 1415 (1985).
[24] B. P. Hu, K. Y. Wang, Y. Z. Wang, Z. X. Wang, Q. W. Yan, P. L. Zhang, and X. D. Sun, Phys. Rev. B **51**, 2905 (1995).